

1
2 **CO₂ and CH₄ exchanges between moist moss tundra and atmosphere on Kapp**
3 **Linne, Svalbard is a net source of CO₂ and CH₄ to the atmosphere**

4 **Anders Lindroth¹, Norbert Pirk², Ingibjörg S Jónsdóttir³, Christian Stiegler⁴, Leif**
5 **Klemedtsson⁵, and Mats B Nilsson⁶**

6 ¹Department of Physical Geography and Ecosystem Science, Lund University, Lund, Sweden.

7 ²Department of Geosciences, University of Oslo, Oslo, Norway.

8 ³Life and Environmental Sciences, University of Iceland, Reykjavik, Iceland.

9 ⁴Bioclimatology, Georg-August Universität Göttingen, Göttingen, Germany.

10 ⁵Department of Earth Sciences, University of Gothenburg, Gothenburg, Sweden.

11 ⁶Department of Forest Ecology and Management, Swedish University of Agricultural Sciences,
12 Umeå, Sweden.

13 Corresponding author: anders.lindroth@nateko.lu.se

Formaterat: Centrerad

14 Abstract

15 We measured CO₂ and CH₄ fluxes using chambers and eddy covariance (only CO₂) from a moist
16 moss tundra in Svalbard. The average net ecosystem exchange (NEE) during the summer (9
17 June-31 August) was negative (sink) with $-0.139 \pm 0.032 - 0.40 \mu\text{mol m}^{-2}\text{s}^{-1} \text{ g C m}^{-2} \text{ day}^{-1}$
18 ~~corresponding to $-11.8 - 37 \text{ g C m}^{-2}$ for the whole summer. The cumulated NEE over the~~
19 whole growing season (day no. 160 to 284) was 24.7 g C m^{-2} due to the
20 losses during the winter. The CH₄ flux during the summer period showed a large spatial and
21 temporal variability. The mean value of all 214 samples was $0.000511 \pm 0.000315 \mu\text{mol m}^{-2}\text{s}^{-1}$
22 which corresponds to a growing season estimate of 0.04 to 0.16 g CH₄ m⁻². Thus, we find that
23 this moss tundra ecosystem is closely in balance with the atmosphere during growing season
24 when regarding exchanges of CO₂ and CH₄. ~~The sink of CO₂ as well as the source of CH₄ are~~
25 small in comparison with other tundra ecosystems in high Arctic. ~~We find that this moss tundra~~
26 emits about 94-100 g CO₂-equivalents m⁻² yr⁻¹ of which CH₄ is responsible for 3.5-9.3% using
27 GWP₁₀₀ of 27.9 respectively GWP₂₀.

29
30 Air temperature, soil moisture and greenness index contributed significantly to explain the
31 variation in ecosystem respiration (R_{eco}) while active layer depth, soil moisture and greenness
32 index were the variables that best explained CH₄ emissions. Estimate of temperature sensitivity
33 of R_{eco} and gross primary productivity (GPP) showed that the sensitivity is slightly higher for
34 GPP than for R_{eco} in the interval 0 – 4.5 °C, thereafter the difference is small up to about 6 °C and
35 then it began to raise rapidly for R_{eco}. The consequence of this, for a small increase in air
36 temperature of 1 degree (all other variables assumed unchanged) was that the respiration
37 increased more than photosynthesis turning the small sink into a small source (4.5 g C m^{-2}) during
38 the growing season. Thus, we cannot rule out that the reason why the moss tundra is close to
39 balance today is an effect of the warming that has already taken place in Svalbard. ~~a modest~~
40 increase in air temperature of 1 degree did not significantly change the NEE during the growing
41 season but that the annual NEE would be even more positive adding another 8.5 g C m^{-2} to the
42 atmosphere. We tentatively suggest that the warming of the Arctic that has already taken place is
43 partly responsible for the fact that the moist moss tundra now is a source of CO₂ to the
44 atmosphere.

45 1 Introduction

46 Climate warming is predicted to be most evident at high latitudes (Friedlingstein et al., 2006)
47 with profound effects on ecosystem functioning. One of the high latitude regions that are
48 expected to experience the most dramatic changes caused by climate change is the Arctic. This
49 region which is located roughly north of the tree-line is characterized by cold winters and cool
50 summers and with mean annual temperatures below zero. The summer periods are short ranging
51 between 3.5 to 1.5 months from the southern boundary to the north and July is normally the
52 warmest month. Annual precipitation is generally low decreasing from about 250 mm in the
53 southern areas to 45 mm in polar deserts in the north (Callaghan et al., 2005).

54
55 The permafrost soils in the Arctic store $1035 \pm 150 \text{ Pg}$ of organic carbon in the top 0-3 m
56 (Hugelius et al., 2014) which is more than the average 2010-2019 of 860 Pg of carbon in the
57 atmosphere (Friedlingstein et al., 2020). The increased warming in these areas can induce higher
58 decomposition rates due to increased microbial activity which will provide a positive feedback to

Formaterat: Inte Upphöjd/ Nedsänkt

59 the climate system (Schuur et al., 2015). On the other hand, warming can also increase
60 photosynthesis and carbon uptake and thus compensate for, or exceed, the effect of increased
61 decomposition. Climate warming is also affecting plant community composition and the length
62 of the growing season (Post et al., 2009) which also has an impact on the processes regulating
63 annual carbon emissions and uptake (Bosiö et al., 2014). There is however a large uncertainty
64 regarding the timing, magnitude and possible sign of potential feedbacks caused by these
65 changes (Myers-Smith et al., 2020).

66
67 Understanding processes that are controlling the exchanges of greenhouse gases in the Arctic is
68 crucial for assessment of potential feedback effects. For this purpose, multiple year-around long-
69 term studies including direct measurements of CO₂ and CH₄ fluxes covering all seasons, winter,
70 spring, summer and autumn would be ideal. This is a great challenge in the harsh climate of the
71 Arctic and with limited support of key infrastructures for, e.g., provision of electricity for
72 operation of instruments.

73
74 In spite of these difficulties a few year-around studies have been performed during the last
75 couple of decades. In the low Arctic, Oechel et al. (2013) demonstrate the importance of the
76 wintertime fluxes in a tussock tundra ecosystem in Alaska. They found that the non-summer
77 season emitted more CO₂ than the corresponding uptake during the summer resulting in a net
78 source to the atmosphere of about 14 g C m⁻² on an annual basis. They also showed that the
79 shoulder seasons, spring and autumn roughly out-weighted the summer uptake. Euskirchen et al.
80 (2012, 2016) measured net CO₂ exchange in three different tundra ecosystems; heath tundra,
81 tussock tundra and wet sedge tundra in northern Alaska over three years. They found that the
82 uptake of -51 to -95 g C m⁻² during the summer (June-August) was overturned by the respiration
83 that occurred during the winter period resulting in net annual losses for all three ecosystems.
84 Zhang et al. (2019) reported five years of year-around flux measurements in a heath ecosystem
85 on west Greenland and they found that the heath was an annual sink of -35±15 g C m⁻². One year
86 with an anomalously deep snow pack showed a 3-fold higher respiration during the winter as
87 compared to the other years which resulted in a significantly lower net uptake during that year.

88
89 Even fewer studies have been done on year-around studies in the high Arctic. Lüers et al. (2014)
90 quantified the annual CO₂ budget using eddy covariance measurements in a river catchment area
91 near Ny-Ålesund on Spitsbergen in the Svalbard archipelago and they found that the ecosystem
92 was in C-balance. The footprint area was a semi-polar desert with only 60% vegetation cover and
93 patches of bare soil and stones. Also in Svalbard but further south in Adventdalen on a flat
94 alluvial fen irregularly covered with ice wedged polygons, Pirk et al. (2017) made year-around
95 measurements of CO₂ fluxes and found it to be a net sink of -82 g C m⁻². Because of the
96 irregularities caused by the ice wedges and the differences in wetness, they focused the analyses
97 on the spatial variability in two different directions, one wetter and one drier, and they estimated
98 the annual net ecosystem exchange to -91 g C m⁻² and -62 g C m⁻² for the respective areas.

99
100 The Arctic ecosystems constitute also a source of CH₄ to the atmosphere even if it is not a very
101 large one. Saunio et al. (2020) estimated that the Northern high latitude region (60°N - 90°N)
102 contributed 4% of global emissions and emissions from wetlands are only part of the emissions
103 from this region. However, in the light of the vulnerability of the high Arctic permafrost areas
104 and considering the large carbon pool and the predicted changes in climate, a quantification and

105 understanding of CH₄ exchanges in these areas are still important. Christensen et al. (2004)
106 showed one example of a dramatic impact of the climate warming on the CH₄ emissions in a
107 permafrost mire in sub-arctic Sweden. The warming which is visible in this area since decades
108 and its impact on permafrost and vegetation changes was estimated to have caused an increase of
109 landscape CH₄ emissions in the range 22-66% in the period 1970 to 2000.

110
111 Mastepanov et al. (2008) were the first to show the importance of emissions also outside of the
112 growing season. They observed a large burst of CH₄ from a fen area in Zackenberg, Greenland
113 after the growing season and during the time when the soil started to freeze. This finding was
114 confirmed in a later paper (Mastepanov et al., 2013) and the process was hypothetically
115 attributed to the subsurface CH₄ pool. Hydrology and vegetation composition play an important
116 role for CH₄ emission and dynamics. McGuire et al. (2012) made a comprehensive summary of
117 CH₄ exchanges of the Arctic tundra showing the difference between wet and dry ecosystems; the
118 wet tundra emitted 5.4 to 13.0 g CH₄-C m⁻² during summer and 8.5 to 20.2 g CH₄-C m⁻²
119 annually. The corresponding values for the dry/mesic tundra were 0.3 to 1.4 g CH₄-C m⁻² and 0.3
120 to 4.3 g CH₄-C m⁻², respectively. Bao et al. (2021) utilized year-around measurements of CH₄
121 fluxes from three sites of the Ameriflux network in Northern Alaska to demonstrate the
122 importance of the spring and autumn seasons for the annual emission. The shoulder seasons
123 contributed about 25% of the annual emissions and the autumn season had about three times
124 higher emission than the spring season. These findings increasingly emphasise the importance of
125 year-around measurements to fully understand the CH₄ controls and dynamics.

126

127 The main aim of this study is to provide another piece of the puzzle concerning CO₂ and CH₄
128 exchanges from different but widespread ecosystem types in the high Arctic. We hypothesise
129 that this moist tundra ecosystem is a net ~~annual~~-carbon sink during the growing season and that
130 the summer emissions of methane will be at ~~average~~-levels comparable with other methane
131 emitting high Arctic ecosystems. We made flux measurements of CO₂ and CH₄ in an moist moss
132 tundra ecosystem situated at Kapp Linne on the west coast of the Svalbard archipelago in 2015
133 and with an additional campaign in 2016. The measurements in 2015 were done using both eddy
134 covariance system (CO₂) and chambers (CO₂ and CH₄) but only chambers in 2016. We quantify
135 ecosystem respiration (R_{eco}), gross primary productivity (GPP) and net ecosystem exchange
136 (NEE) during the growing season based on a combination of chamber end eddy covariance
137 ~~measurements and we extend the time period to a full year by modelling~~. The CH₄ emission was
138 only quantified for the summer season. We also analyze the environmental controls of the fluxes.

139 2 Materials and Methods

140 2.1 Research site and measurements

141

142 This study was performed in the Svalbard archipelago near the weather station Isfjord Radio
143 (78°03'08" N 13°36'04" E, alt. 7 m) which is located right on the foreland of Kapp Linné on the
144 island of Spitzbergen (Fig. S1). The tundra area where the measurements were performed is
145 located about 1 km southeast of the station. The study area consists of moist moss tundra, a
146 widespread ecosystem in Svalbard (Vanderpuye et al., 2002; Ravolainen et al., 2020). The
147 vegetation is characterised by the moss species *Tomentypnum nitens*, *Sanionia uncinata* and
148 *Aulacomium palustre* and a sparse cover of vascular plants (20-40%), dominated by *Equisetum*

149 *arvense*, *Salix polaris* and *Bistorta vivipara*. Other vascular plant species found in the plots:
150 *Saxifraga cespitosa*, *Saxifraga oppositifolia*, *Silene acaulis*, and some grass species, most likely
151 *Alopecurus ovatus* (previously *A. borealis*), and *Poa arctica*. The vegetation analysis was made
152 from photographs of chamber location plots taken between 26 June and 2 July 2015 (see Figs.
153 S4a-4y in Supplement).

154
155 The net ecosystem exchange of CO₂ was measured with an eddy covariance (EC) system located
156 centrally on the moss tundra (78°03'28.6" N 13°38'40" E). The sonic anemometer (USA-1;
157 Metek GmbH, Germany) was mounted on top of a tripod (see Fig. S1) at 2.7 m height. The CO₂
158 and H₂O concentrations were measured with an open path sensor (LI-7500; Li-Cor Inc., USA)
159 placed just beneath the sonic and inclined about 30° pointing towards east. Radiation
160 components, incoming and outgoing short-wave and long-wave (CNR-4; Kipp & Zonen, the
161 Netherlands) were measured at 2.0 m height above ground with the sensor directed towards
162 south. All sensors were connected to a datalogger (CR-1000; Campbell Scientific, USA) which
163 was powered by a solar panel and a battery. The EC sensors were sampled and stored at 10 Hz
164 and all other sensors were sampled at 0.1 Hz with storage of 30 min mean values. These
165 measurements were made from 25 June to 17 September 2015. The total data coverage during
166 this period was 47% with a longer break in the measurements between 28 July and 29 August.

167
168 The soil efflux of CO₂ and CH₄ was measured with a dark chamber connected to a gas analyzer
169 (Ultraportable Greenhouse Gas Analyzer; Los Gatos Research, USA) on 24 locations within the
170 EC average footprint area. A circular thin-steel frame, 15 cm in diameter and 15 cm high, was
171 inserted ca 5 cm into the ground in each location. The sharp edge of the frames made it easy to
172 insert them into the ground without damaging the vegetation and with minimal soil disturbance.
173 A picture was taken of each frame (see Supplement) for documentation of vegetation and for
174 calculation of different indexes. The chamber was also made from steel and it had a rubber seal
175 in the end facing the frame (Fig. S2) to make it air tight when mounted on the frame. The volume
176 of the chamber and the part of the frame raised above the surface was 5.3 L. A small fan was
177 installed inside the chamber to provide good mixing of the air during measurement. A small
178 weight (stone) was placed on top of the chamber during measurement to prevent it from moving
179 due to wind gusts. During concentration measurement air was circulated in a closed loop
180 between the chamber and the gas analyzer in ca. 10 m long 4 mm diameter polyethylene tubes (see
181 Fig. S2). The air flow through the analyzer was ca 1.2 L min⁻¹. The chamber was ventilated in
182 the free air about 1 minute before each measurement which lasted for 5 minutes. The
183 concentrations were recorded and stored once per second by the gas analyzer. The time stamp of
184 the recorded data was used to identify measurement cycles for analysis of fluxes.

185
186 The chamber measurement positions were selected in the following way. The frames were
187 grouped in two sections, one north-east and one south-west of the flux tower since it was
188 expected that the main wind direction would be along that direction. Each group was then split
189 into three subsections with four measurement points within each one of them. The locations were
190 named S1:1-S1:4, S2:1-S2:4, S3:1-S3:4, N1:1-N1:4, N2:1-N2:4 and N3:1-SN3:4. The four
191 measurement points within each subsection were then placed along a transect with 3-4 m
192 between each point. This way it was possible to measure all four chamber locations without
193 having to move the whole measurement system. Chamber measurements were made in three
194 separate campaigns: mid-summer (26 June to 2 July 2015), late-summer (25-27 August 2015)

195 and early-summer (14-15 June 2016). Each location was measured three times during each one
196 of the three campaigns, a total of 216 measurements. Besides gas concentrations, also soil
197 temperature (5 cm), soil moisture (0-5 cm) and active layer depth was measured during each
198 campaign.

199
200 Meteorological data needed for analyses and gap-filling were obtained as follows: Hourly air
201 temperature and relative humidity from Isfjord radio, half-hourly global radiation from
202 Adventdalen, daily snow depth and ground ice conditions from Svalbard airport and monthly
203 precipitation from Isfjord radio and Barentsburg. The distance between the measurement site and
204 these stations are; Isfjord radio, 1 km, Barentsburg, 13 km, Svalbard airport, 46 km and
205 Adventdalen, 50 km. Using data from the more distant locations, Svalbard airport and
206 Adventdalen, introduces some additional uncertainty. Concerning global radiation data we could
207 compare in situ measured half-hourly radiation with the corresponding data from Adventdalen
208 for a shorter period and it showed general good agreement although with relatively large scatter
209 ($y = 0.84x + 15.9$; $r^2=0.57$; $n=580$). According to Dobler et al. (2021) the amount of precipitation
210 in the area where Kapp Linne and Svalbard airport are located don't show any significant
211 differences on an annual basis. Vickers et al. (2020) analysed timing of snow cover in Svalbard
212 and they show that the mean (2000-2019) first snow-free day is very similar in areas where Kapp
213 Linne and Svalbard airport are located. Thus, we are confident that using data from these
214 relatively remote locations does not introduce serious bias in our analyses. Data sources are
215 given in Acknowledgement.

Formaterat: Teckensnitt:12 pt

Formaterat: Teckensnitt:12 pt

Formaterat: Teckensnitt:12 pt

Formaterat: Teckensnitt:12 pt

216 217 **3. Data analysis**

218
219 The rawdata from the eddy covariance flux measurements were analysed using the Eddypro
220 software version 6.1.0 (Li-Cor, 2016). Correction was made for the impact of the additional heat
221 flux in the sensor path of the open path analyzer on the flux calculations according Burba et al.
222 (2008). Gap filling during the measurement period was made using the REddyProc online eddy
223 covariance data processing tool developed at the Max Planck Institute for Biogeochemistry
224 (Wutzler et al., 2018) without u^* correction since we could not identify any threshold for u^* . The
225 u^* threshold is generally low for low and smooth vegetation (Pastorello et al., 2020) and for a
226 wind exposed site as ours, it is not surprising that such threshold could not be found. Flux
227 partitioning was made with the daytime-based method according Lasslop et al. (2000). Only data
228 of highest quality, i.e. class=0 was retained for the gap filling and further analyses. Gap filling
229 outside of the EC measurement period to obtain the carbon balance for a full growing season~~year~~
230 was made using empirical relationships for R_{eco} and GPP (see below).

231
232 For flux footprint calculations the roughness length (z_0) is needed and it was calculated from the
233 wind profile relationship in near neutral ($-0.01 < z/L < 0.01$) conditions:

$$234$$
$$235 z_0 = \frac{z_m}{e^{(u(z) \frac{k}{u^*})}} \quad (1)$$

236
237 where z_m is measurement height, $u(z)$ is wind speed at height z , k is von Karman's constant and
238 u^* is friction velocity. We used the flux footprint prediction (FFP) online tool by Kjün et al.
239 (2015) to calculate the footprint climatology.

240

241 The fluxes from the chamber measurements were estimated from the time change of the
 242 concentrations using linear regression. Every individual measurement was inspected and
 243 evaluated manually. These inspections showed that 50 seconds for CO₂ and 100 seconds for CH₄
 244 were optimal to obtain near perfectly linear responses a few seconds after the chamber had been
 245 placed on the frame. The slopes of the regressions were then used to calculate fluxes per unit
 246 surface area. The flux detection limits for CO₂ and CH₄ were calculated in the following way:
 247 first the peak-to-peak variation in the respective gases were determined when the chamber was
 248 ventilated in the free air and when conditions were steady. Then 20 sets of artificial ‘fluxes’ for
 249 each gas species were estimated based on 100 randomly generated concentrations for each data
 250 set. The peak-to-peak difference was used as seed (input) for the randomly generated values. The
 251 95% value of the distribution of these randomly generated fluxes was taken as the flux detection
 252 limit for the respective gas.

253
 254 The pictures of the vegetation inside of the chamber frames were analysed using the ImageJ
 255 (<https://imagej.net>) public domain software. The camera color channel information (digital
 256 numbers for Red (R), Green (G) and Blue (B) channels) was collected from the JPEG pictures.
 257 This type of pictures is for instance used in studies that are tracking the phenological
 258 development of vegetation (e.g. Richardson et al., 2009). The so-called green index (GI) is
 259 applied to detect differences in greenness of vegetation:

$$260 \quad GI = G/(R+G+B) \quad (2)$$

261
 262
 263 This index was also estimated for the central footprint area (100 m radius) of the flux
 264 measurement location using a picture taken at 160 m above the altitude of the measurement area.

265 Forward stepwise linear regression (Sigmaplot 12.5) was used to analyze the dependency of the
 266 CO₂ and CH₄ fluxes on environmental variables. We tested for air temperature (T_a), soil moisture
 267 (θ), soil temperature (T_s), active layer depth (ALD), measurement location (S_{id}) and GI.

268
 269 For gap filling of R_{eco} we only had access to air temperature with full annual coverage and, thus,
 270 we could only use this driver for estimation of the R_{eco}. The measured chamber CO₂ fluxes were
 271 fitted to the Lloyd & Taylor (1994) model with air temperature (T_a) as independent variable:

$$272 \quad FCO_2 = a \cdot e^{b \left(\frac{1}{56.02} - \frac{1}{T_a + 46.02} \right)} \quad (3)$$

273
 274
 275 During the EC measurement period (25 June to 17 September 2015) the GPP was estimated as:

$$276 \quad GPP = NEE_f - R_{eco} \quad (4)$$

277
 278
 279 Where NEE_f is the gap filled NEE according to Wutzler et al. (2018). This way R_{eco} and GPP
 280 become consistent with the measured and gap filled NEE. For the time before and after this
 281 period NEE was estimated as the sum of modelled R_{eco} and modelled GPP. The data for the GPP
 282 model was derived from:

$$283 \quad GPP_m = NEE_m - R_{eco} \quad (5)$$

284
 285

286 Where NEE_m is the measured net ecosystem exchange. The GPP_m was then fitted to a light
287 response function:

288
289
$$GPP_m = c1 + c2 \cdot c3 / (c2 + R_g) \quad (6)$$

290

291 **4 Results**

292 For CO_2 exchanges and partitioning we combined the soil efflux measurements with the chamber
293 system with the eddy covariance flux measurements. This was crucial for the partitioning and for
294 gap filling because from 20 April to 20 August at this location the sun is above the horizon 24
295 hours of the day and this means that there were few occasions of dark nighttime measurements
296 with the eddy covariance system and all of these were collected at the very end of the summer.
297 We consider the chamber measurements that were distributed across the summer to be more
298 representative of R_{eco} for this location.

299

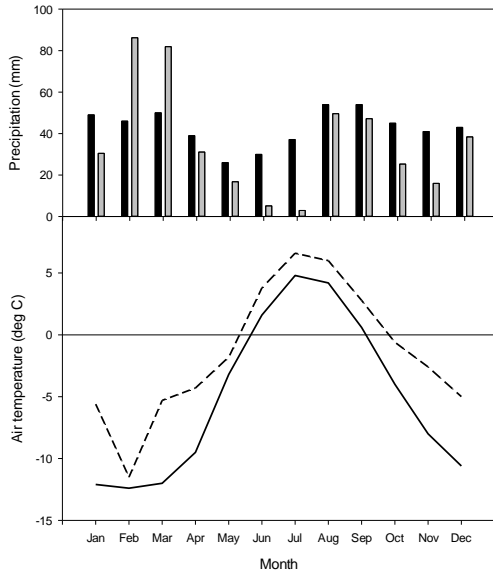
300 For CH_4 exchanges we don't have any eddy covariance measurements so we present only
301 chamber data for this variable.

302

303 4.1 Weather

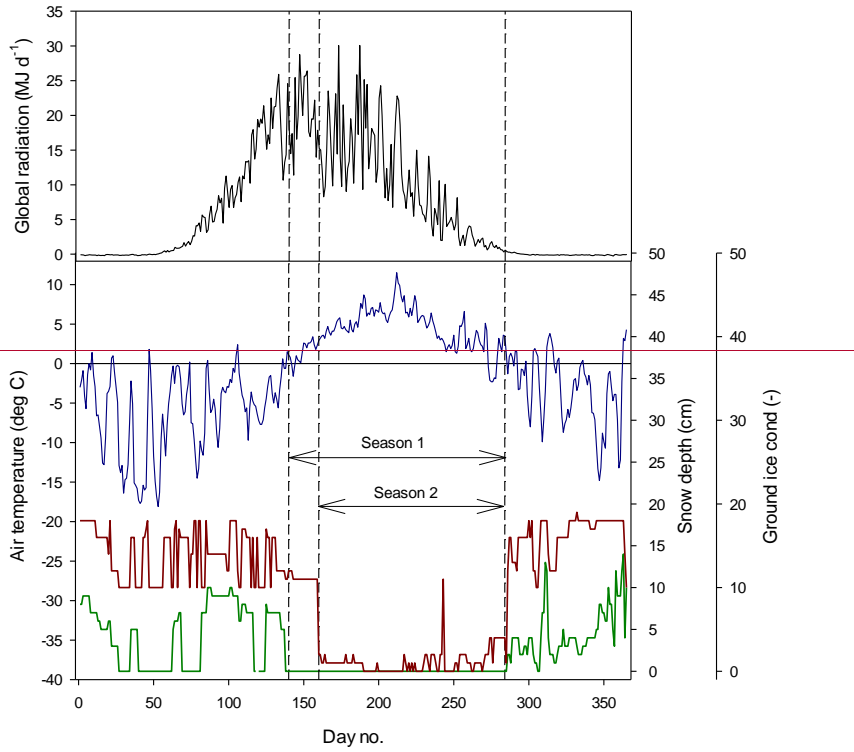
304

305 The mean annual temperature at Kapp Linne was $-1.5^\circ C$ during 2015 which was $3.5^\circ C$ higher
306 than the long-term mean (1961-1990) of $-5.1^\circ C$. The summer (June-August) mean of $5.5^\circ C$ was
307 $2.0^\circ C$ higher than the long-term mean for the same time period (Fig. 1). The summer
308 precipitation in 2015 was much lower, 58 mm as compared to the long-term precipitation which
309 was 121 mm. The annual precipitation was also lower, 431 mm compared to the long-term
310 precipitation which was 514 mm.

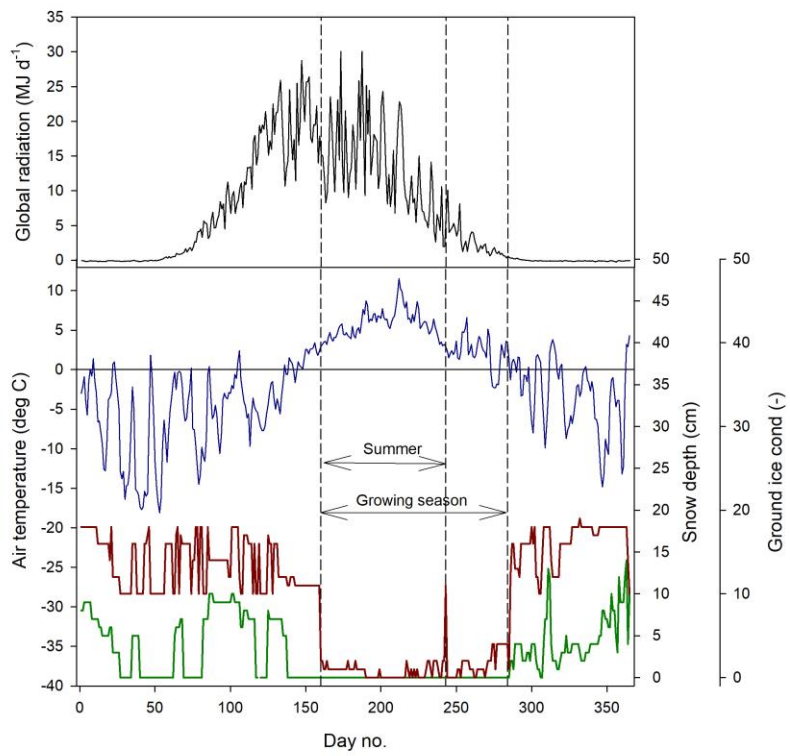


311 Figure 1. Monthly precipitation (top): Long-term average 1961-1990 black bars and 2015 grey
 312 bars. Data from Barentsburg for January-May, from Isfjord Radio for June-December. Mean
 313 monthly air temperature (bottom): Solid line is long-term average 1961-1990 and dotted line is
 314 2015. Data from Isfjord Radio which is located about 1 km west of the investigation area.
 315

316
 317 We defined the start of the growing season (the period during which vegetation is
 318 photosynthesizing) in two different ways. The first (denoted Season 1, day no. 140; see Fig. 2)
 319 based on when daily air temperature started to stay above zero more steadily and the second
 320 based on the permanence of the snow pack which resulted in start day no. 160 and end day no.
 321 284 (Fig. 2). The summer period which normally is defined as June through August was here
 322 defined as lasting between 9 June (same as start of growing season) until end of August
 323 (Fig. 2), (denoted Season 2, day no. 160) when most of the snow had disappeared. The ending of
 324 the growing season was defined as when the air temperature fell more steadily below zero, when
 325 ground ice began to establish and when a significant snow pack was established (day no. 284;
 326 Fig. 2).



327

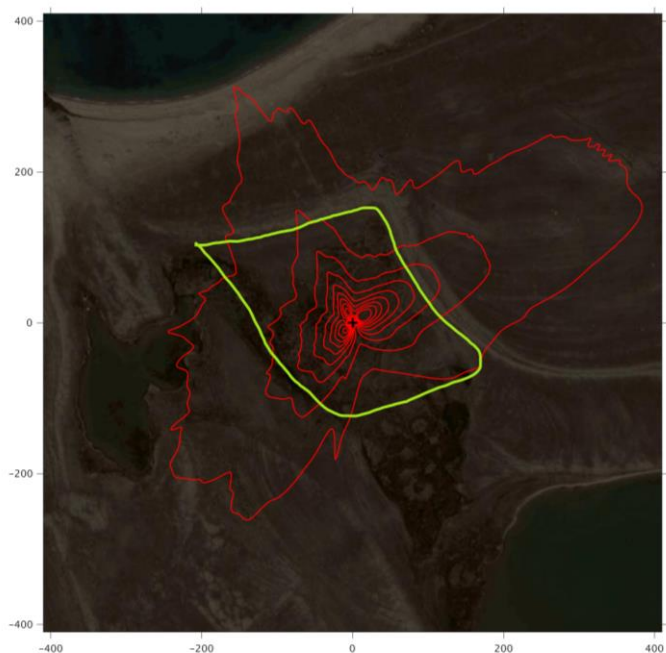


328
329

330 Fig. 2 Weather conditions during 2015. Top panel: Mean daily global radiation at Adventdalen.
331 Bottom panel: Mean daily air temperature at Isfjord Radio (blue), snow depth (red) and ground
332 ice conditions (green) at Svalbard airport close to Longyearbyen. The ground ice condition is
333 scaled from 0 to 20 where 0 is no snow or ice on the ground and 20 indicate a complete cover of
334 snow or ice.

335 4.2 Flux footprint and greenness

336
337 The footprint climatology shows a good representativity of the moss tundra surface by the EC
338 measurements with 60-70% of fluxes emanating from areas well within the border of the tundra
339 (Fig. 3). The mean green index for a circular area with radius of 100 m centered at the flux tower
340 was 0.34 which corresponded exactly to the mean value for all chamber locations. The GI for the
341 24 chamber locations varied between 0.316 and 0.369. We observed a good (visual) correlation
342 between GI and coverage of green plants (see Figures S4a-S4y of chamber location pictures and
343 GI).
344
345

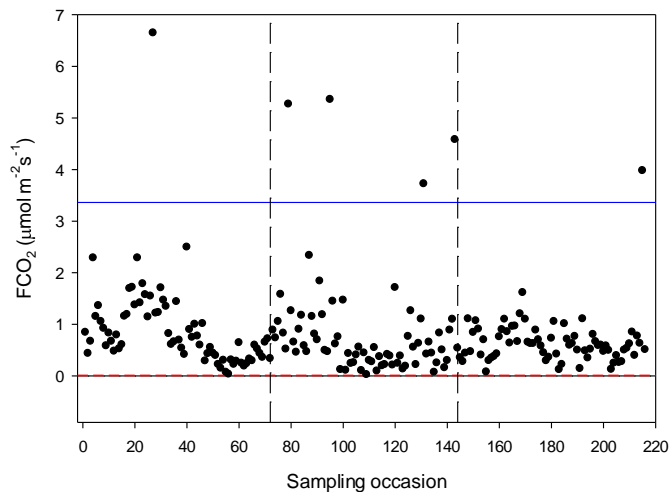


346
347 Figure 3. The footprint climatology with red contour lines 10-90%. The area within the green
348 line mark the heart of the moss tundra. The scale (m) is shown on the outer borders of the
349 picture.

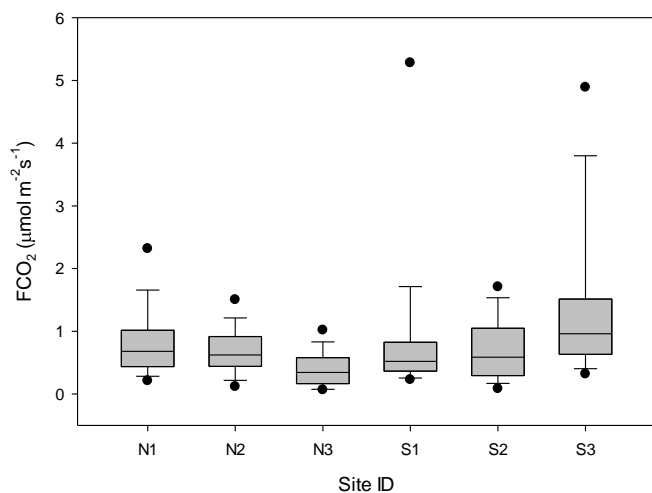
350 4.3 CO₂ exchanges

352

353 The CO₂ fluxes from the chamber measurements showed quite large variation over time (Fig. 4)
354 and across sampling locations (Fig. 5). The mean CO₂ flux of all samples was 0.81±0.11 μmol
355 m⁻²s⁻¹. The uncertainty is given as the 95 confidence limit.
356



357
358 Figure 4. Measured CO₂ exchange (FCO_2) from the 24 sampling points using dark chamber and
359 portable gas analyzer. The dashed red line indicates CO₂ flux detection limit and the blue line
360 represents 3xS.D. of all data points. The dashed vertical lines separate sampling periods from left
361 to right: 14-15 Juneearly summer, 26 June – 2 Julymid summer and 25-27 August,
362 respectivelylate summer.



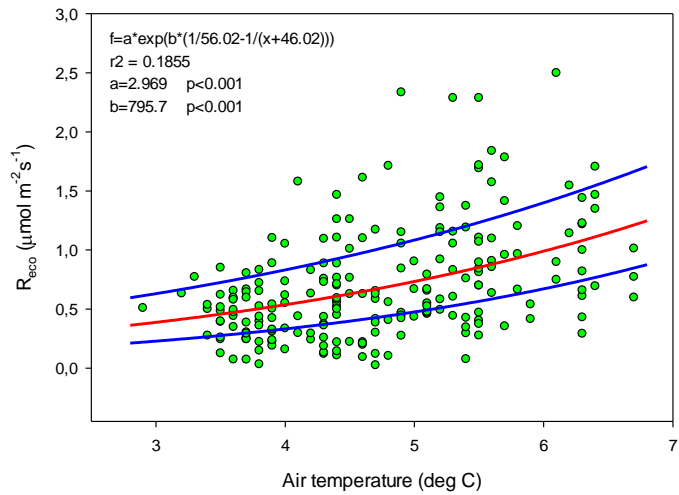
363
 364 Figure 5. Box plot of CO₂ fluxes (FCO_2) per sampling location named N1-N3, S1-S3. The
 365 boundaries of the grey boxes represent the 25% and 75% percentiles, the line represent the
 366 median, whiskers above and below the boxes indicate the 10% and 90% percentiles. Outlying
 367 points are also shown.

368
 369 Of the tested environmental variables T_a , θ , T_s , ALD, S_{id} and GI it was only T_a , θ and GI that
 370 contributed positively and significantly in decreasing order to explain the variability of the CO₂
 371 flux (Table 1).

372
 373 Table 1. Result of stepwise linear regression with CO₂ flux as dependent variable. Normality test
 374 failed but significance in all variables was confirmed with Wilcoxon Signed rank tests. T_a is air
 375 temperature, θ is soil moisture and GI is green index.

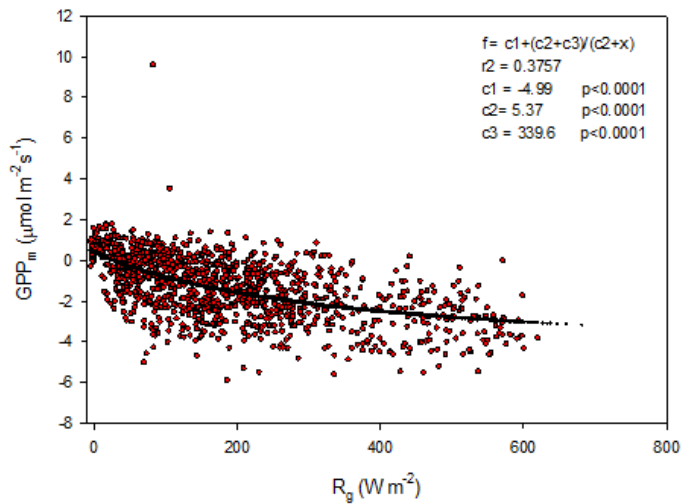
Variable	Partial- R ²	Probability (p)
T_a	0.190	<0.001
θ	0.037	0.002
GI	0.023	0.002

376
 377
 378 Ideally all of these variables should be used in a model to estimate R_{eco} for gap filling purposes
 379 but we could only use air temperature since this was the only variable that we had access to with
 380 complete coverage for a full year. The Lloyd & Taylor model (Eq. 3 & Fig. 6)) was thus used to
 381 estimate ecosystem respiration for 2015 using half-hourly air temperature as input.



382
 383 Figure 6. Measured ecosystem respiration (R_{eco} ; green dots) plotted against air temperature. The
 384 red curve is the fitted equation and the blue curves are the corresponding boundaries when
 385 considering the standard deviation of the parameters.
 386

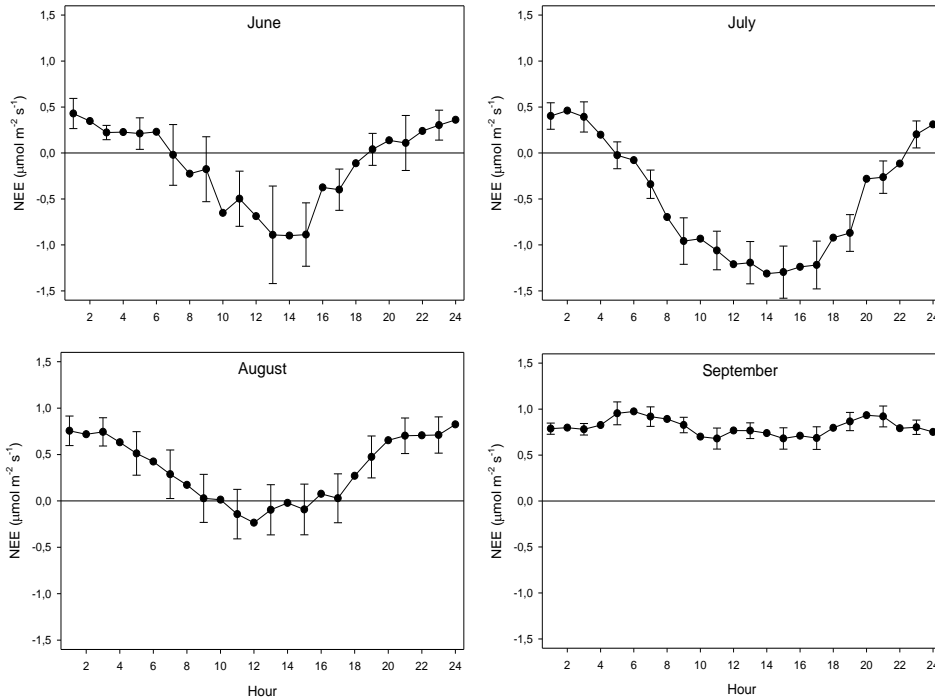
387 The modelled gross primary productivity (Eq. 6; GPP_m) had a small offset when global radiation
 388 was zero (Fig. 7). This offset was adjusted for when the model was applied for gapfilling so that
 389 GPP become zero during nighttime.



390
391
392 Figure 7. Gross primary productivity (GPP_m) plotted against global radiation (R_g); red symbols
393 are estimated values according to eq. (5) and the black symbols are the fitted model.

394
395 ~~We assumed that GPP was zero for the periods outside of the growing season and that our R_{eeo}~~
396 ~~model was valid during winter as well as during growing season. However, during winter the air~~
397 ~~temperature is not the appropriate driver for respiration because of the insulating effect of the~~
398 ~~snow cover. We did not have access to soil temperature from our site but data from Adventdalen~~
399 ~~which is located about 60 km east from our site, showed that the soil surface temperature was~~
400 ~~close to zero degrees below the snow pack during the winter (N. Pirk, unpublished data). Thus,~~
401 ~~we assumed that the situation would be similar in our site and used zero degrees as driver for~~
402 ~~respiration.~~

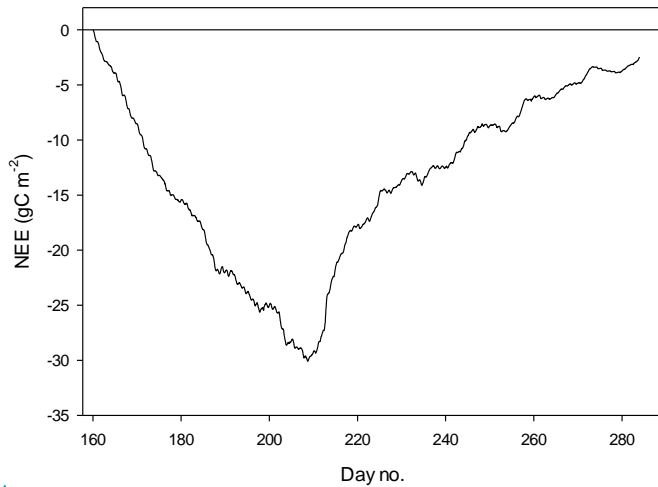
403
404
405



406 Figure 8. The mean monthly diurnal course of net ecosystem exchange (NEE) during the period
 407 of eddy covariance measurements 25 June to 17 September. The error bars (every 2nd shown) are
 408 the 95% confidence interval. Notice that the main part of August was gap filled because of
 409 measurement problems.

Formaterat: Upphöjd

411
 412
 413 The diurnal course of NEE during June - August exhibit the normal pattern with a successively
 414 increasing drawdown of CO₂ during first half of the day resulting in a maximum around noon. It
 415 should be noted that during June until 20 August the sun was over the horizon 24 hours, thus no
 416 dark period. The positive values at the beginning and end of the diurnal courses are a result of
 417 R_{eco} being larger than GPP. As pointed out in Fig. 8, most of the data of August were gapfilled
 418 causing some additional uncertainty. However, the diurnal course seems reasonable although the
 419 peak during noon is much lower as compared to July. This can be explained by the much lower
 420 incoming radiation in August as compared to July; the mean global radiation in July was 192 W
 421 m⁻² and 98 W m⁻² in August. The mean air temperature was similar during July and August. In
 422 September the incoming radiation is very low and thus GPP is also very low which result in a
 423 NEE that is dominated by the R_{eco}. The positive NEE values around mid-night during June –
 424 September are in good accordance with the values from the independent dark chamber
 425 measurements (Fig. 5).



427 Figure 9. The cumulated half-hourly net ecosystem exchange (NEE) during growing season.

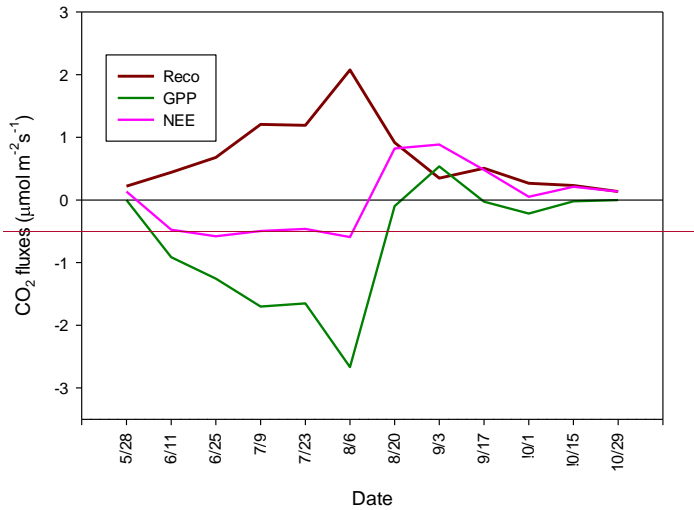
428
429
430 The mean net CO₂ flux during the growing season was $-0.019 \pm 0.024 \mu\text{mol m}^{-2}\text{s}^{-1}$ with
431 uncertainty given as the 95% confidence limit. The cumulated NEE during growing season
432 ended up negative with -2.5 g C m^{-2} (Fig. 9). The mean net CO₂ flux during summer was -
433 $0.139 \pm 0.032 \mu\text{mol m}^{-2}\text{s}^{-1}$ (95% confidence limit) and the cumulated NEE was -11.8 g C m^{-2}
434 (Table 2).

435 The mean bi-weekly fluxes show that NEE is negative from about one week into June until one
436 week into August (Fig. 8). The mean NEE is relatively constant during this period with a low -
437 $0.5 \mu\text{mol m}^{-2}\text{s}^{-1}$. The maximum bi-weekly GPP is about $2.5 \mu\text{mol m}^{-2}\text{s}^{-1}$ while the corresponding
438 R_{eco} is about $2.0 \mu\text{mol m}^{-2}\text{s}^{-1}$. The GPP become positive during one period in the autumn
439 indicating an underestimation of R_{eco} during that time.

440

Ändrad fältkod

Formaterat: Inte Upphöjd/ Nedsänkt



441 Figure 8. Bi-weekly gap filled CO₂ fluxes for season 2 (see Fig. 2) at Tunsjömyren, Kapp Linne
 442 during 2015.
 443
 444

445 The annual modelled and gap filled NEE was negative, -12.4 g C m⁻² for season 1 and positive,
 446 24.7 g C m⁻² for season 2. The gapfilled NEE (Table 2) during the summer (June-August) was
 447 37 g C m⁻² or -0.40 g C m⁻² day⁻¹ which is good agreement with the measured NEE (25 June-31
 448 August) with a mean daily uptake of -0.40 g C m⁻² day⁻¹. A summary of all components for the
 449 different seasons are presented in Table 2.
 450

451 Table 2. Summary of ~~annual and~~ seasonal C-fluxes from Kapp Linne. R_{eco} is ecosystem
 452 respiration, GPP is gross primary productivity and NEE is net ecosystem exchange.
 453

Period	Component	Value (gC m ⁻²)
Growing season	Reco	110.2
	GPP	-112.7
	NEE	-2.5
Summer	Reco	94.1
	GPP	-105.9
	NEE	-11.8

← Formaterad tabell

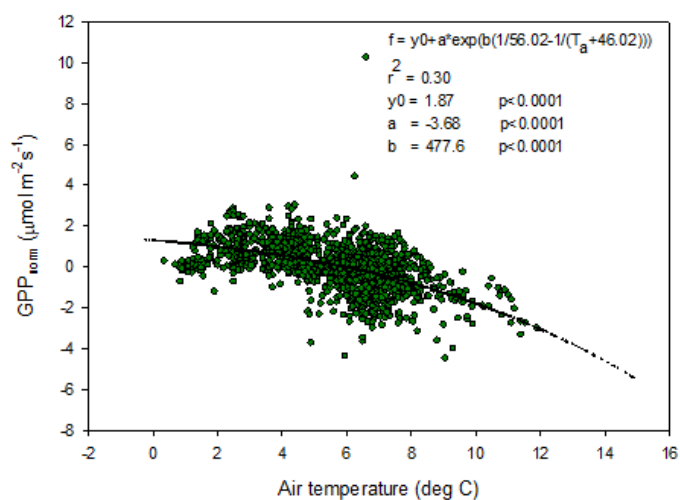
← Formaterat: Centrerad

← Formaterat: Vänster

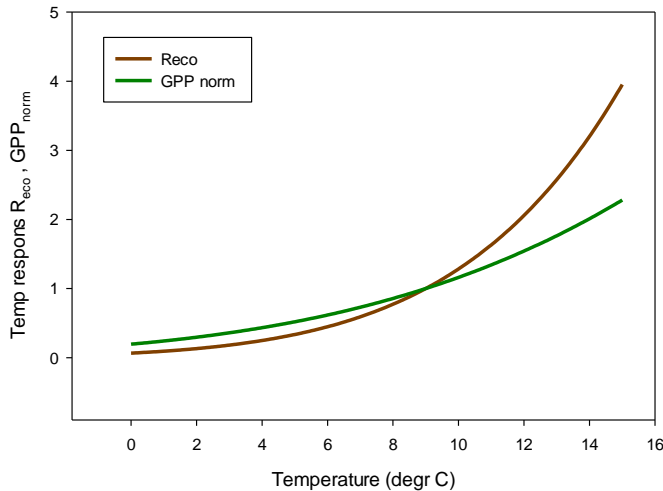
454
 455 4.4 Temperature sensitivity of R_{eco} and GPP
 456

457 The temperature sensitivity of the R_{eco} is already given by the fitted Lloyd & Taylor (1994)
 458 equation. In the absence of long time series of measurements during multiple year were natural
 459 climate variability could be used to assess temperature sensitivity of GPP we approached this

460 problem in the following way. We normalize GPP for its dependence on radiation by estimating
 461 the difference between the ‘measured’ GPP and the model which only depends on radiation (see
 462 Fig. 7). A stepwise linear regression with normalized GPP as dependent variable and air
 463 temperature, time of season and vapour pressure deficit as independent variables, showed that of
 464 the total explained variance, air temperature stood for 94% and time of season and vapour
 465 pressure deficit for 3% each. Thus, the resulting normalized GPP show effectively a dependence
 466 on air temperature (Fig. 109) with values becoming more negative, i.e. showing increasing GPP
 467 with increasing temperature. We fitted the same type of model to these data as for the R_{eco} to be
 468 able to compare sensitivities to temperature.



469 Figure 109. Normalized gross primary productivity (GPP) plotted against air temperature and
 470 with the fitted exponential model.
 471
 472



473 Figure 110. Temperature sensitivity for ecosystem respiration (R_{eco}) (brown) and R_g -normalized
 474 (positive) gross primary productivity (GPP) (green).
 475

476
 477 In Fig. 110 we reversed the sign of the GPP temperature response function to make it more easily
 478 comparable with the R_{eco} response model. The temperature sensitivity ($\mu\text{mol m}^{-2}\text{s}^{-1} \text{K}^{-1}$) can be
 479 estimated from the slope of these curves and the sensitivity is slightly higher for GPP than for
 480 R_{eco} in the interval 0 – 4.5 °C, thereafter the difference is small up to about 6.7 °C then it began to
 481 raise rapidly for R_{eco} . We tested what impact this could have by increasing the measured half-
 482 hourly air temperature by 1 °C and found that during the growing season (season 2) the GPP
 483 increased by -31.989 g C m⁻² and R_{eco} by 36.453 g C m⁻². Thus, a slightly larger minor-increase
 484 of R_{eco} GPP-as compared to -GPP R_{eco} -resulting in that the small sink of -2.5 g C m⁻² turns into a
 485 source of 4.5 g C m⁻². However, a one degree higher winter temperature resulted in an addition
 486 respiration of 9 g C m⁻². Thus, an estimated loss of 8.5 g C m⁻² for the whole year.
 487

488 4.5 CH₄ exchanges

489
 490 The CH₄ fluxes from the chamber measurements showed large variation over time (Fig. 124) and
 491 across sampling locations (Fig. 132). The mean CH₄ flux of all samples was 0.00051 ± 0.00024
 492 $\mu\text{mol m}^{-2}\text{s}^{-1}$. The uncertainty is given as the 95% confidence limit. Setting all fluxes that fell
 493 within the flux detection limits to zero changed the mean value with -0.2%. Assuming that the
 494 mean flux was representative for the whole of growing season 1, the total CH₄ summer emission
 495 was 0.039 to 0.164 g CH₄ m⁻². Converting this to CO₂-equivalents (CO₂-eq) we get a range of 1.1
 496 to 4.6 g CO₂-eq for the summer and if we add also a possible winter emission of 22% of the
 497 annual (following Bao et al., 2021) we obtain an annual mean of 3.2±2.0 g CO₂-eq using a
 498 GWP₁₀₀ of 27.9 (Arias et al., 2021). The corresponding value using GWP₂₀ of 81.2 (Arias et al.,
 499 2021) is 9.3±5.8 g CO₂-eq for the annual emission.
 500

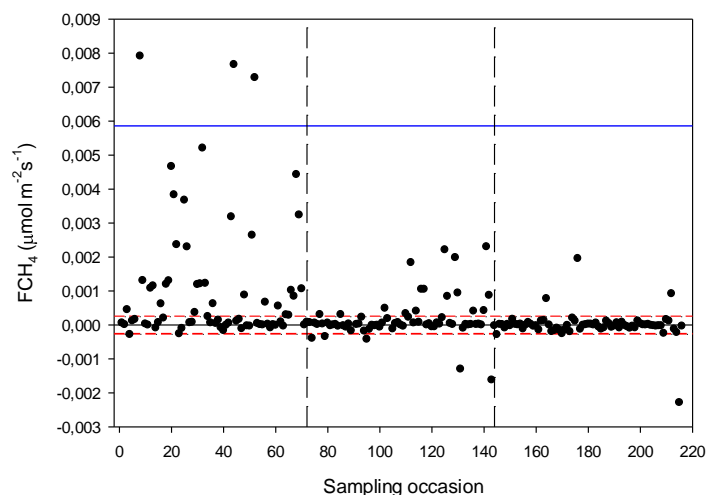
501 We also noticed a clear trend during the summer with highest fluxes in mid-June and then
 502 decreasing during the following two sampling occasions. The respective mean values with 95%
 503 confidence intervals for the three sampling periods were $0.00121 \pm 0.000512 \mu\text{mol m}^{-2}\text{s}^{-1}$ (June 14-
 504 15), $0.000332 \pm 0.000465 \mu\text{mol m}^{-2}\text{s}^{-1}$ (June 26- July 2) and $-0.00000781 \pm 0.0000936 \mu\text{mol m}^{-2}\text{s}^{-1}$
 505 ¹(August 25-26).

506
 507 For CH_4 exchanges we found *ALD*, θ and *GI* to contribute significantly to explain the variance of
 508 the flux (Table 3). The CH_4 flux responded negatively to increasing *ALD* and positively to θ and
 509 *GI*.

510
 511 Table 3. Result of stepwise multiple linear regression with CH_4 flux as dependent variable.
 512 Normality test failed but significance in all variables was confirmed with Wilcoxon Signed rank
 513 tests. ALD is active layer depth, θ is soil moisture and GI is green index.

Variable	Delta-R ²	Probability (p)
ALD	0.175	<0.001
θ	0.025	0.01
GI	0.020	0.004

515
 516



517
 518 Figure 124. Measured CH_4 exchange (F_{CH_4}) from the 24 sampling points using dark chamber
 519 and portable gas analyzer. The dashed red lines indicate CH_4 flux detection limit, (i.e. inside the
 520 limits of detection the exact numbers are highly uncertain) and the blue line represents $3 \times \text{S.D.}$
 521 The dashed vertical lines – same as in Fig. 4.

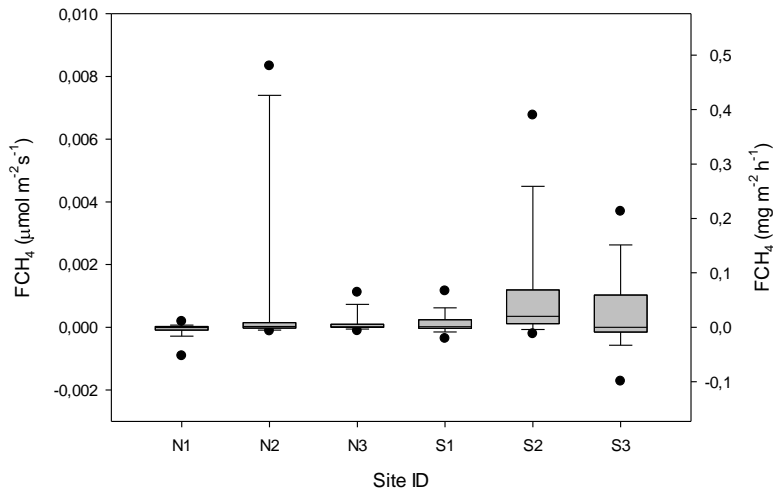


Figure 132. Box plot of CH₄ fluxes (F_{CH_4}) per sampling location named N1-N3, S1-S3. The statistics includes also the data that fall within the flux detection limits. The boundaries of the grey boxes represent the 25% and 75% percentiles, the line represent the median, whiskers above and below the boxes indicate the 10% and 90% percentiles. Outlying points are also shown.

5 Discussion

5.1 Annual and seasonal CO₂ fluxes

We focus our discussion mainly on comparison with other tundra sites located in the North Atlantic area since these sites are influenced by the North Atlantic Current with its impact on weather patterns and climate. This limits the comparisons to sites in Greenland, Svalbard and Northern Scandinavia. However, we broaden the comparison a bit by adding two sites from Alaska.

~~Our annual NEE was in the range -12.4 to 24.7 $g\ C\ m^{-2}$ depending on definition of growing season (Table 2). We judge the latter value to be more realistic since season 1 includes an unrealistically high GPP when there is still a snow cover on the ground in early spring. We used the high and low estimates of the fitted functions for R_{eco} (see Fig. 6) to assess the sensitivity of annual NEE to uncertainty in winter respiration and we found the range to be between -17.1 $g\ C\ m^{-2}$ to 32.9 $g\ C\ m^{-2}$.~~

Lund et al. (2012) found that the start of the uptake period was strongly correlated with start of the snowmelt for the fen in Zackenberg, NE Greenland. They defined the start of snowmelt as the day when snow depth was <0.1 m. This coincides very well with our definition of start of growing season 2 (see Fig. 2). Our results for the growing season NEE showing a small net uptake of -2.5 $g\ C\ m^{-2}$ is at the low end in comparison with any other high arctic sites which all

548 ~~show a larger gain of carbon during the growing seasons. Soegaard and Nordstroem (1999)~~
549 ~~reported an annual NEE of -64.4 g C m^{-2} for the fen in Zackenberg and Pirk et al. (2017)~~
550 ~~reported -82 g C m^{-2} for an alluvial fen in Adventdalen, Svalbard, not far from Kapp Linne. For a~~
551 ~~site on the west coast of Greenland, Disco island with heath vegetation, Zhang et al. (2019)~~
552 ~~reported an annual NEE of $-25 \pm 15 \text{ g C m}^{-2}$. Christensen et al. (2012) reported a range of -20 to $-$~~
553 ~~95 g C m^{-2} for annual NEE in a palsa mire in Abisko, Northern Sweden. Our results are closer to~~
554 ~~the values found for a sparsely vegetated catchment area in Bayelva, Ny Ålesund were Lüers et~~
555 ~~al. (2014) reported annual NEE to be 0 g C m^{-2} . If we go beyond the North Atlantic area to the~~
556 ~~low Arctic region in North America we can find sites that has a positive NEE on annual basis,~~
557 ~~13.6 g C m^{-2} for a tussock tundra near Atkasuk, Alaska (Oechel et al., 2013) and $21-61 \text{ g C m}^{-2}$~~
558 ~~for a heath and $2-82 \text{ g C m}^{-2}$ for a wet sedge ecosystem in Imnavait creek (Eurkirchen et al.,~~
559 ~~2012).~~

560
561 Lund et al. (2012) analysed 10 years of EC flux measurements from a heathland in Zackenberg
562 and they reported a NEE range of -39.7 to -4.3 g C m^{-2} for the growing season. ~~Our result for the~~
563 ~~growing season NEE of -6.8 g C m^{-2} (Season 2; Table 2) fall within the same range but it~~
564 ~~was only two years out of ten that showed NEE values close to zero but still indicating a small net~~
565 ~~uptake that low uptake in Zackenberg heath. Their measured growing season GPP was in the~~
566 ~~range of -95.4 to -54.1 g C m^{-2} and the R_{eco} was in the range of 37.7 to 63.8 g C m^{-2} . Our~~
567 ~~corresponding values were -112.7 to -6.3 g C m^{-2} for GPP and 110.2 to 109.5 g C m^{-2} for R_{eco} . López-~~
568 ~~Blanco et al. (2017) presented data over a period of eight years of EC flux measurements from~~
569 ~~Kobbefjord, SW Greenland over an area of mixed fen and heath vegetation. Their growing~~
570 ~~season ranges were; for NEE -74.2 to -45.9 g C m^{-2} , for GPP -316.2 to $-181.8 \text{ g C m}^{-2}$ and for~~
571 ~~R_{eco} it was 144.2 to 279.2 g C m^{-2} excluding 2011 which was anomalous because of a pest~~
572 ~~outbreak and 2014 which did not have a full growing season.~~

573
574 ~~Our EC measurements estimate of a small summer (June-August) NEE of -11.8 to -37 g C m^{-2}~~
575 ~~(Table 2) is also different in comparison with other tundra sites which show larger uptake during~~
576 ~~the summer; in between ranges reported for a fen type of vegetation in NE Greenland, Soegaard~~
577 ~~and Nordstroem (1999) reported; -96.3 g C m^{-2} while Rennermalm et al. (2005) reported~~
578 ~~(Soegaard and Nordstroem 1999) to -50 g C m^{-2} for the same site but for a different~~
579 ~~year. (Rennermalm et al. 2005). Groendahl et al. (2007) reported a range of and heath vegetation;~~
580 ~~-1.4 to -18.9 g C m^{-2} for heath vegetation also on NE Greenland (Groendahl et al. 2007).~~

581
582 It is difficult to compare growing season values firstly because they are rarely defined the same
583 way. Only small differences in definition of start and end of growing season can have a large
584 impact on the NEE values since NEE is the sum of two large components of almost equal size
585 and of different sign. ~~In our case a 20 days difference in the beginning of the season changes~~
586 ~~growing season NEE from -12.4 to 24.7 g C m^{-2} . Secondly, it is also difficult to compare GPP~~
587 ~~and R_{eco} for any season since the methods to split NEE into components differ from case to case.~~
588 ~~The most reliable comparison is probably for summer season (June – August) since most studies~~
589 ~~represents this period best in terms of measurement coverage and quality. And thirdly, there are~~
590 ~~differences in vegetation type that can have a big impact on gas exchanges. Our moist moss~~
591 ~~tundra is dominated by moss species and mosses are not as efficient primary producers as~~
592 ~~vascular plants and this make the net uptake of carbon dioxide small as compared to heath or wet~~
593 ~~fen systems. So, with this in mind we are pretty confident with placing the C exchange rates of~~

594 ~~the moss tundra intermediate between fen and heath type of vegetation in the North Atlantic~~
595 ~~region.~~

596
597 The climate warming is predicted to be most evident at high latitudes such as the Arctic region.
598 Svalbard has experienced significant warming during the last decades (1971-2017) with 3- 5
599 degrees with the largest increase in the winter and smallest in the summer (Hanssen-Bauer et al.,
600 2019). Our air temperature observations in 2015 are in line with these results (Fig.1). An
601 interesting question is if such changes in temperature has also affected the net carbon balance of
602 the ecosystem? Our analysis of temperature sensitivity of R_{eco} and GPP shows that this could be
603 the case for this site since R_{eco} is increasing more than GPP for temperatures above about 6 °C
604 which occurs quite frequent during the summer (see Fig. 2). Our analyses of the impact of a
605 temperature increase of 1 °C showed that our small sink of -2.5 g C m^{-2} during growing season
606 would be turned into a similarly small source of 4.5 g C m^{-2} for a 1 degree increase in air
607 temperature. These results are in line of those of Welker et al. (2004) who performed a warming
608 experiment in high Arctic tundra ecosystems. They showed that the net ecosystem exchange in
609 the wet tundra ecosystem decreased by 20% during growing season under a 2 degree warming
610 treatment. This was in contrast to the dry and mesic ecosystems which increased their net carbon
611 uptake by 12-30%.

612 613 614 5.2 CH₄ fluxes 615

616 Our estimated growing season CH₄ flux of 0.08 g C m^{-2} is very low compared to most other
617 methane emitting tundra sites; the Zackenberg fen site emitted CH₄ in the range 1.4 to 4.9 g C m^{-2}
618 (Mastepanov et al. (2013), Jackowicz-Korczynski et al. (2010) and Jammet et al. (2015)
619 reported 20.1 to $25.1 \text{ g CH}_4 \text{ m}^{-2}$ for the Stordalen mire in Northern Sweden. For three different
620 sites in northern Alaska, Bao et al. (2021) reported annual emissions between 1.8 and 8.5 g CH_4
621 m^{-2} which corresponds to 0.94 and $4.5 \text{ g CH}_4 \text{ m}^{-2}$ for the growing season based on their estimate
622 that growing season emissions are 52.6% of the annual emissions. Sachs et al. (2008) measured
623 CH₄ exchanges with EC method in a northern Siberian polygon tundra and found generally low
624 fluxes of about $18.5 \text{ mg CH}_4 \text{ m}^{-2} \text{ day}^{-1}$ with little variation over the growing season. This rate
625 adds up to $2.3 \text{ g CH}_4 \text{ m}^{-2}$ for their four months long growing season.
626

627 It should be pointed out that we did not perform measurements during the shoulder seasons
628 meaning that we probably underestimate the seasonal total. Importance of shoulder seasons was
629 first pointed out by Mastepanov et al. (2008) which discovered a large burst of CH₄ at and after
630 the onset of soil freezing. One interesting observation is that the main part of our CH₄ flux
631 occurred during the sampling period 14-15 June 2016 which is about 30 days after snow melt.
632 This is the time of the season when CH₄ emissions normally are peaking (Mastepanov et al.
633 2013). After that, the rates dropped to practically zero in late August (see Fig. 1~~2~~4).
634

635 ~~If we sum up the annual net CO₂ and CH₄ fluxes expressed as CO₂-eq we find that the moss~~
636 ~~tundra is emitting in total $60 \text{ g CO}_2\text{-eq}$ of which the methane stands for 7%. So even if the CH₄~~
637 ~~fluxes are small, it still represents a significant global warming impact in relative terms.~~
638

639 The comparison between the different sites are hampered by the fact that they in most cases
640 belong to different bioclimatic subzones with differences in climate and vegetation (Walker et
641 al., 2005). The only site besides Kapp Linne that belong to subzone B is the one in Ny Ålesund.
642 The other high Arctic sites Adventdalen and Zackenberg both belong to subzone C, the
643 intermediate high/low Arctic sites Kobbefjord and Disco Island belongs to subzone D
644 respectively C/D. The low Arctic site Atqasuk belong to subzone D and the Imnavait Creek
645 belong to subzone E. The sub-Arctic Abisko is not classified by Walker et al. (2005) but based
646 mean July air temperature it should belong to subzone E. These differences in climate and
647 vegetation should be kept in mind when comparing results from different sites.

649 5.3 Environmental controls of fluxes

650
651 A key issue in high Arctic is how ecosystems with soil that contain large amounts of frozen
652 carbon will respond to warming. A recent report about the future climate of Svalbard (Hanssen-
653 Bauer et al. 2019) show that appalling changes are at risk to occur. By 2071-2100 compared to
654 1971-2000 the mean annual temperature is estimated to increase by 7 °C to 10 °C for the medium
655 and high emission scenarios, respectively. Precipitation is also estimated to increase by 45%
656 respectively 65% for these scenarios. Such large changes will of course also have a lot of other
657 impacts as well for instance shorter snow season, more erosion and sediment transport, changes
658 in vegetation composition and growth etc etc. Assessment of such large changes are very
659 difficult and is far beyond the scope of this paper. We have however shown that for a smaller
660 temperature increase of 1 degree, the impact on the net carbon balance during the growing
661 season will be minute; the increase in ecosystem respiration is compensated for by a
662 corresponding, or actually slightly larger increase of gross primary productivity. Similar
663 compensation effect was obtained for a heath site in Zackenberg by Lund et al. (2012). They
664 used multi-year measurements to assess the effect of changes in temperature on the growing
665 season fluxes. ~~But, if we also consider an increase in temperature during winter, it is most likely
666 that the annual NEE becomes weakened. It is not unlikely that the impact of climate change with
667 higher temperature that is already a reality in Svalbard can be the reason why the annual NEE
668 now is positive, i.e. the moss tundra is a GHG source of CO₂ to the atmosphere.~~

669
670 We found that air temperature was the main control of ecosystem respiration followed by soil
671 moisture and greenness index (Table 1). We had expected that soil temperature should contribute
672 significantly to explain the variations in R_{eco} but it did not. Cannone et al. (2019) showed that
673 ground surface temperature at 2 cm depth contributed significantly to explain R_{eco} in nearby
674 Adventdalen during early, peak and late parts of the growing season. In their study soil moisture
675 was also significant during peak and late seasons. One possible explanation to this difference in
676 responses could be that our soil temperature was measured at 5 cm depth and that air temperature
677 was more representative for the microbial processes taking place in or near the soil surface.
678 Interestingly, GI contributed significantly to explain variations in R_{eco} . The GI was clearly
679 correlated with the abundance of *Salix polaris* (see Supplement) and thus we interpret the
680 positive correlation between GI and R_{eco} to be an effect of increasing contribution by autotrophic
681 respiration to the total respiration.

682 We found no significant correlation between CH₄ emission and temperature. The best
683 explanation was by active layer depth followed by soil moisture and GI (Table 3). But it should
684 be pointed out that ALD and θ are not independent from each other and that ALD can be

685 regarded as a proxy for any seasonal variability, like plant phenology. Soil moisture decreases
686 with increasing active layer depth. The correlation between GI and CH₄ emission is probably
687 also connected with abundance of [the vascular plant *Salix polaris*](#) ~~which is a vascular plant.~~
688 Vascular plants are since long mentioned as a pathway for CH₄ from the soil interior to the
689 atmosphere in wet tundra ecosystems (e.g. Schimel, 1995) but it could also be an effect of
690 mediation of soil by the root exudation of organic acids as mentioned by Ström et al. (2012).
691 However, we have not found any studies supporting the latter hypothesis concerning *Salix*
692 *polaris*.

693 **6 Conclusions**

694 Our analyses of EC and chamber flux measurements have shown that the moss tunda on Kapp
695 Linne is a small ~~sink~~ ~~source~~ of CO₂ and ~~an even smaller~~ source of CH₄ ~~during on an the growing~~
696 ~~season annual basis.~~ Realizing that the winter season also emit CO₂, we tentatively conclude that
697 this moist moss tundra is a source on an annual basis. Concerning the magnitude of the CO₂
698 exchanges during summer we find it to be anomalous compared to in-between those of fens and
699 heath ecosystems located in the North Atlantic region which all are sinks during the summer.
700 The CH₄ exchange is much lower than for other tundra ecosystems in the region.

701
702 The temperature sensitivity for CO₂ exchange was slightly higher for GPP than for R_{eco} in the
703 low temperature range of 0–4.5 °C, almost similar up to ~~6~~ 7 °C and thereafter it was considerably
704 higher for R_{eco}. The consequence of this, for a small increase in air temperature of 1 degree (all
705 other variables assumed unchanged) was that the respiration increased more than photosynthesis
706 turning the small sink into a small source in the two fluxes practically evened out during the
707 growing season. But a warmer winter period would probably also result in an additionally
708 increased loss of carbon. We cannot rule out that the reason why the moss tundra is close to
709 balance a net source today is an effect of the warming that has already taken place in Svalbard.

710 The analysis of which environmental factors that controlled the small-scale fluxes showed that
711 air temperature dominated for R_{eco} and active layer depth for CH₄ but we also found that
712 greenness index significantly explained part of the variation in these fluxes. For R_{eco} we
713 attributed this to an increased share of autotrophic respiration to the total and for CH₄ we
714 hypothesized that the abundance of the ~~dwarfwoody~~ shrub *Salix polaris* effected the exchange
715 either through internal plant pathway for methane or through increased provision of C substrate
716 to the anaerobic microbial community stimulating the production of methane. This finding is an

717 indication that modeling of CO₂ as well as of CH₄ fluxes can be improved by also considering
718 differences and changes in greenness of the vegetation.

719 **7 Supplement**

720 The supplement contains some additional photographs of equipment, site and color photographs
721 of vegetation within the frames used for chamber measurements.

722 **8 Data availability**

723 Data can be obtained from [https://zenodo.org \(10.5281/zenodo.5704508\)](https://zenodo.org/10.5281/zenodo.5704508).

724 **9 Author contribution**

725 AL designed the study and wrote the manuscript. NP and AL performed the EC measurements
726 and analysed the EC data. ISJ did the vegetation characterization. AL, CS, LK and MBN
727 performed the chamber measurements. All authors have read and commented the manuscript.

728 **10 Competing interests**

729 We declare no competing interests.

730 **11 Acknowledgments**

731 This work did not receive any other funding except salaries for the authors from their respective
732 organizations. Observations of air temperature, relative humidity, precipitation, ground ice
733 conditions and snow depth were obtained from Norwegian Centre for Climate Services (NCCS)
734 and provided under licence CC BY 4.0. Global radiation data from Adventdalen was obtained
735 from the University Centre in Svalbard (UNIS). Thanks to associated professor Jonas Åkerman,
736 Lund University for support with information about the site.
737

738 **12 References**

739 Arias, P. A., Bellouin, E., Coppola, R.G. et al.: Technical Summary, in: *Climate Change 2021:*
740 *The Physical Science Basis. Contribution of Working Group I to the Sixth Assessment*
741 *Report of the Intergovernmental Panel on Climate Change*, edited by: Masson-Delmotte,
742 V., P. Zhai, A. Pirani, S. L. Connors, C. Péan, S. Berger, N. Caud, Y. Chen, L. Goldfarb,
743 M. I. Gomis, M. Huang, K. Leitzell, E. Lonnoy, J.B.R. Matthews, T. K. Maycock, T.
744 Waterfield, O. Yelekçi, R. Yu and B. Zhou, Cambridge University Press, In Press, 2021.

745 Bao, T., Xu, X., Jia, G., Billesbach, D.P. and Sullivan, R.C.: Much stronger tundra methane
746 emissions during autumn freeze than spring thaw, *Global Change Biology*, 27, 376–387,
747 [https://doi.org/ 10.1111/gcb.15421](https://doi.org/10.1111/gcb.15421), 2021

748 Bosiö, J., Stiegler, C., Johansson, M., Mbufong, H. N. and Christensen, T. R.: Increased
749 photosynthesis compensates for shorter growing season in subarctic tundra—8 years of
750 snow accumulation manipulations, *Climatic Change*, 127, 321–334,
751 <http://doi.org/10.1007/s10584-014-1247-4>, 2014.

- 752 Burba, G. G., McDermitt, D., Grelle, A., Anderson, D.J. and Xu, L.: Addressing the influence of
 753 instrument surface heat exchange on the measurements of CO₂ flux from open-path gas
 754 analyzers, *Global Change Biology*, 14, 1854–1876, [https://doi.org/10.1111/j.1365-](https://doi.org/10.1111/j.1365-2486.2008.01606.x)
 755 [2486.2008.01606.x](https://doi.org/10.1111/j.1365-2486.2008.01606.x), 2008.
- 756 Callaghan, T.V., Björn, L.O., Chapin III, F.S., Chernov, Y., Christensen, T.R., Huntley, B., Ims,
 757 R., Johansson, M., Jolly Riedlinger, D., Jonasson, S., Matveyeva, N., Oechel, W.,
 758 Panikov, N. and Shaver, G.: Arctic tundra and polar desert ecosystems, in: *Arctic Climate*
 759 *Impact Assessment*, edited by: ACIA, Cambridge University Press, 243-352, 2005.
- 760 Cannonea, N., Pontib, S., Christiansen, H.H., Christensen, T.R., Pirk, N. and Guglielmin, M.:
 761 Effects of active layer seasonal dynamics and plant phenology on CO₂ land atmosphere
 762 fluxes at polygonal tundra in the High Arctic, *Svalbard, Catena*, 174, 142-153,
 763 <https://doi.org/10.1016/j.catena.2018.11.013>, 2019.
- 764 Christensen, T.R., Johansson, T., Akerman, H.J. and Mastepanov, M.: Thawing sub-arctic
 765 permafrost: Effects on vegetation and methane emissions, *Geophysical Research Letters*,
 766 31, L04501, <https://doi.org/10.1029/2003GL018680>, 2004.
- 767 Christensen, T.R., Jackowicz-Korzynski, M., Aurela, M., Crill, P., Heliasz, M., Mastepanov, M.
 768 and Friborg, T.: Monitoring the Multi-Year Carbon Balance of a Subarctic Palsa Mire
 769 with Micrometeorological Techniques, *Ambio*, 41, 207–217,
 770 <https://doi.org/10.1007/s13280-012-0302-5>, 2012.
- 771 [Dobler, A., Lutz, J., Landgren, O. and Haugen, J. E.: Circulation Specific Precipitation Patterns](#)
 772 [over Svalbard and Projected Future Changes, *Atmosphere*, 11, 1378;](#)
 773 [doi:10.3390/atmos11121378, 2021.](#)
- 774
- 775 Euskirchen, E. S., Bret-Harte, M. S., Scott, G. J., Edgar, C., and Shaver, G. R.: Seasonal patterns
 776 of carbon dioxide and water fluxes in three representative tundra ecosystems in northern
 777 Alaska, *Ecosphere*, 3, 1–19, <https://doi.org/10.1890/ES11-00202.1>, 2012.
- 778
- 779 Euskirchen, E.S., Bret-Harte, M.S., Shaver, G.R., Edgar, C.W., and Romanovsky, V.E.: Long-
 780 Term Release of Carbon Dioxide from Arctic Tundra Ecosystems in Alaska, *Ecosystems*,
 781 20, 960–974, <http://doi.org/10.1007/s10021-016-0085-9>, 2017.
- 782 Friedlingstein, P., Cox, P., Betts, R., Bopp, L., von Bloh, W., Brovkin, V., Cadule, P., Doney, S.,
 783 Eby, M., Fung, I., Bala, G., John, J., Jones, C., Joos, F., Kato, T., Kawamiya, M., Knorr,
 784 W., Lindsay, K., Matthews, H. D., Raddatz, T., Rayner, P., Reick, C., Roeckner, E.,
 785 Schnitzler, K. G., Schnur, R., Strassmann, K., Weaver, A. J., Yoshikawa, C., and Zeng,
 786 N.: Climate-carbon cycle feedback analysis: Results from the C4MIP model
 787 intercomparison, *J. Climate*, 19, 3337–3353, <https://doi.org/10.1175/JCLI3800.1>, 2006.

Formaterat: Engelska (USA)

Formaterat: Teckensnitt:12 pt

Formaterat: Teckensnitt:12 pt

Formaterat: Engelska (USA)

Formaterat: Indrag: Vänster: 0 cm, Första raden: 0 cm

- 822 Lund, M., Falk, J. M., Friborg, T., Mbufong, H. N., Sigsgaard, C., Soegaard, H., and Tamstorf,
823 M. P.: Trends in CO₂ exchange in a high Arctic tundra heath, 2000–2010, *J. Geophys.*
824 *Res.- Biogeo.*, <https://doi.org/10.1029/2011JG001901>, 2012.
- 825 Lüers, J., Westermann, S., Piel, K., and Boike, J.: Annual CO₂ budget and seasonal CO₂
826 exchange signals at a high Arctic permafrost site on Spitsbergen, Svalbard archipelago,
827 *Biogeosciences*, 11, 6307–6322, <http://doi.org/10.5194/bg-11-6307>, 2014.
- 828 Mastepanov, M., Sigsgaard, C., Dlugokencky, E. J., Houweling, S., Strom L., Tamstorf, M. P.,
829 and Christensen, T. R.: Large tundra methane burst during onset of freezing, *Nature*, 456,
830 628–631, <http://doi.org/10.1038/nature07464>, 2008.
- 831 Mastepanov, M., Sigsgaard, C., Tagesson, T., Ström, L., Tamstorf, M. P., Lund, M., and
832 Christensen, T. R.: Revisiting factors controlling methane emissions from high-Arctic
833 tundra, *Biogeosciences*, 10, 5139–5158, <https://doi.org/10.5194/bg-10-5139-2013>, 2013.
- 834 McGuire, A. D., Christensen, T. R., Hayes, D., Heroult, A., Euskirchen, E., Kimball, J. S.,
835 Koven, C., Lafleur, P., Miller, P. A., Oechel, W., Peylin, P., Williams, M., and Yi, Y.: An
836 assessment of the carbon balance of Arctic tundra: comparisons among observations,
837 process models, and atmospheric inversions, *Biogeosciences*, 9, 3185–3204,
838 <https://doi.org/10.5194/bg-9-3185-2012>, 2012.
- 839 Myers-Smith, I. H., Kerby, J. T., Phoenix, G. K., Bjerke, J. W., Epstein, H. E., Assman, J. J.,
840 John, C., Adreu-Hayles, L., Angers-Blondin, S., Beck, P. S. A., Berner, L. T., Bhatt, U.
841 S., Bjorkman, A. D., Blok, D., Bryn, A., Christiansen, C. T., Cornelissen, J. H. C.,
842 Cunliffe, A. M., Elmendorf, S. C., Forbes, B. C., Goetz, S. J., Hollister, R. D., de Jong,
843 R., Loranty, M. M., Marcias-Fauria, K., Maseyk, K., Normand, S., Olofsson, J., Parker,
844 T. C., Parmentier, F.-J. W., Post, E., Schaepman-Strub, G., Stordal, F., Sullivan, P. F.,
845 Thomas, H. J. D., Tømmervik, H., Treharne, R., Tweedie, C. E., Walker, D. A.,
846 Wilmking, M. and Wipf, S.: Complexity revealed in the greening of the Arctic, *Nat.*
847 *Clim. Chang.*, 10, 106–117, <https://doi.org/10.1038/s41558-019-0688>, 2020.
- 848 Oechel, W. C., C. A. Laskowski, G. Burba, B. Gioli, and Kalhori, A.A.M.: Annual patterns and
849 budget of CO₂ flux in an Arctic tussock tundra ecosystem, *J. Geophys. Res. Biogeosci.*,
850 119, 323–339, <http://doi.org/10.1002/2013JG002431>, 2014.
- 851 Pastorello, G., Trotta, C., Canfora, E. et al.: The FLUXNET2015 dataset and the ONEFlux
852 processing pipeline for eddy covariance data, *Sci Data*, 7, 225,
853 <https://doi.org/10.1038/s41597-020-0534-3>, 2020.
- 854 Pirk, N., Sievers, J., Mertes, J., Parmentier, F.-J. W., Mastepanov, M., and Christensen, T. R.:
855 Spatial variability of CO₂ uptake in polygonal tundra: assessing low-frequency
856 disturbances in eddy covariance flux estimates, *Biogeosciences*, 14, 3157–3169,
857 <https://doi.org/10.5194/bg-14-3157-2017>, 2017.

858 Post, E., Forchhammer, M. C., Bret-Harte, M. S., Callaghan, T. V., Christensen, T. R., Elberling,
859 B., Fox, A. D., Gilg, O., Hik, D. S., Høye, T. T., Ims, R. A., Jeppesen, E., Klein, D. R.,
860 Madsen, J., McGuire, A. D., Rysgaard, S., Schindler, D. E., Stirling, I., Tamstorf, M. P.,
861 Tyler, N. J. C., van der Wal, R., Welker, J., Wookey, P. A., Schmidt, M. and Astrup, P.:
862 Ecological dynamics across the arctic associated with recent climate change, *Science*,
863 325, 1355–1358, <http://doi.org/10.1126/science.117311>, 2009.

864 Ravolainen, V., Soininen, E. M., Jónsdóttir, I. S., Eischeid, I., Forchhammer, M., van der Wal,
865 R. and Pedersen, A. Ø.: High Arctic ecosystem states: Conceptual models of vegetation
866 change to guide long-term monitoring and research, *Ambio*, 49, 666–677,
867 <https://doi.org/10.1007/s13280-019-01310-x>, 2020.

868 Rennermalm, A.K., Soegaard, H., and Nordstroem, C.: Interannual Variability in Carbon
869 Dioxide Exchange from a High Arctic Fen Estimated by Measurements and Modeling,
870 *Arctic, Antarctic, and Alpine Research*, 37(4), 545-556, [https://doi.org/10.1657/1523-0430\(2005\)037\[0545:IVICDE\]2.0.CO;2](https://doi.org/10.1657/1523-0430(2005)037[0545:IVICDE]2.0.CO;2), 2005.

872 Richardson, A. D., Braswell, B. H., Hollinger, D. Y., Jenkins, J. P. and Ollinger, S. V.: Near-
873 surface remote sensing of spatial and temporal variation in canopy phenology, *Ecological*
874 *Applications*, 19, 1417–1428, <http://doi.org/10.1890/08-2022.1>, 2009.

875 Sachs, T., Wille, C., Boike, J., and Kutzbach, L.: Environmental controls on ecosystem-scale
876 CH₄ emission from polygonal tundra in the Lena river delta, Siberia, *J. Geophys. Res.-*
877 *Biogeosci.*, 113, G00A03, <http://doi.org/10.1029/2007JG000505>, 2008.

878 Saunio, M., Stavert, A.R., Poulter, B et al.: The global methane budget 2000-2017, *Earth Syst.*
879 *Sci. Data*, 12, 1561–1623, <https://doi.org/10.5194/essd-12-1561>, 2020.

880 Schimel, J.P.: Plant Transport and Methane Production as Controls on Methane Flux from Arctic
881 Wet Meadow Tundra, *Biogeochemistry*, 28 (3), 183-200,
882 <https://doi.org/10.1007/BF02186458>, 1995.

883 Schuur, E. A. G., McGuire, A. D., Schadel, C., Grosse, G., Harden, J. W., Hayes, D. J.,
884 Hugelius, G., Koven, C. D., Kuhry, P., Lawrence, D. M., Natali, S. M., Olefeldt, D.,
885 Romanovsky, V. E., Schaefer, K., Turetsky, M. R., Treat, C. C., and Vonk, J. E.: Climate
886 change and the permafrost carbon feedback, *Nature*, 520, 171–179,
887 <https://doi.org/10.1038/nature14338>, 2015.

888 Soegaard, H. & Nordstroem, C.: Carbon dioxide exchange in a high-arctic fen estimated by eddy
889 covariance measurements and modeling, *Glob. Change Biol.*, 5, 547–562,
890 <https://doi.org/10.1111/j.1365-2486.1999.00250.x>, 1999.

891 Strom, L., Tagesson, T., Mastepanov, M., and Christensen, T. R.: Presence of *Eriophorum*
892 *scheuchzeri* enhances substrate availability and methane emission in an Arctic wetland,
893 *Soil Biol. Biochem.*, 45, 61–70, <http://doi.org/10.1016/j.soilbio.2011.09.005>, 2012.

894

- 895 Walker, D. A., Raynolds, M. K., Daniëls, F. J. A., Einarsson, E., Elvebakk, A., Gould, W. A.,
896 Katenin, A. E., Kholod, S. S., Markon, C. J., Melnikov, E. S., Moskalenko, N. G., Talbot,
897 S. S., Yurtsev, B. A. and the other members of the CAVM Team: The Circumpolar
898 Arctic vegetation map, *Journal of Vegetation Science*, 16, 267-282,
899 <https://doi.org/10.1111/j.1654-1103.2005.tb02365.x>, 2005.
- 900 [Welker, J.M., Fahnestock, J.T., Henry, G.H.R., O'Dea, K.W. and Chimner, R.A.: CO₂ exchange](#)
901 [in three Canadian High Arctic ecosystems: response to long-term experimental warming.](#)
902 [Global Change Biology, 10, 1981-1995. Doi: 1011/j.1365-2486.2004.00857.x, 2004.](#)
903
- 904 Vanderpuye, A. W., Elvebakk, A. and Nilsen, L.: Plant communities along environmental
905 gradients of high-arctic mires in Sassendalen, Svalbard, *J. Veg. Sci.*, 13, 875–884,
906 <http://doi.org/10.1111/j.1654-1103.2002.tb02117.x>, 2002.
- 907
- 908 [Vickers, H., Karlsen, S. R. and Malnes, E.: A 20-Year MODIS-Based Snow Cover Dataset for](#)
909 [Svalbard and Its Link to Phenological Timing and Sea Ice Variability, Remote Sens., 12,](#)
910 [1123; doi:10.3390/rs12071123, 2020.](#)
911
- 912
- 913 Wutzler, T., Lucas-Moffat, A., Migliavacca, M., Knauer, J., Sickel, K., Šigut, L., Menzer, O. and
914 Reichstein, M.: Basic and extensible post-processing of eddy covariance flux data with
915 REddyProc, *Biogeosciences*, 15(16), 5015-5030, Doi:10.5194/bg-15-5015-2018, 2018.
- 916 Zhang, W., Jansson, P-E., Sigsgaard, C., McConnella, A., Jammet, M.M., Westergaard-Nielsen,
917 A., Lund, M., Friborg, T., Michelsen, A., and Elberling, B.: Model-data fusion to assess
918 year-round CO₂ fluxes for an arctic heath ecosystem in West Greenland (69°N),
919 *Agricultural and Forest Meteorology*, 272-273, 176-186,
920 <https://doi.org/10.1016/j.agrformet.2019.02.021>, 2019.

Formaterat: Engelska (USA)

Formaterat: Teckensnitt:12 pt

Formaterat: Indrag: Vänster: 0 cm, Första raden: 0 cm